Accepted Manuscript

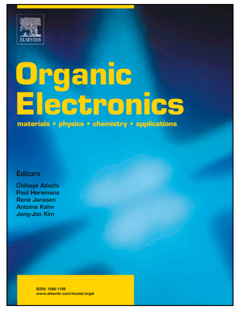

Solution processible imidazole-based iridium dendrimers with oligocarbazole for nondoped phosphorescent OLEDs

Mingming Zhang, Xuefei Li, Shumeng Wang, Junqiao Ding, Lixiang Wang

PII: S1566-1199(19)30086-2

DOI: https://doi.org/10.1016/j.orgel.2019.02.017

Reference: ORGELE 5123

To appear in: *Organic Electronics*

Received Date: 2 November 2018

Revised Date: 21 January 2019

Accepted Date: 11 February 2019

Please cite this article as: M. Zhang, X. Li, S. Wang, J. Ding, L. Wang, Solution processible imidazole-based iridium dendrimers with oligocarbazole for nondoped phosphorescent OLEDs, *Organic Electronics* (2019), doi: https://doi.org/10.1016/j.orgel.2019.02.017.

Graphic Abstract

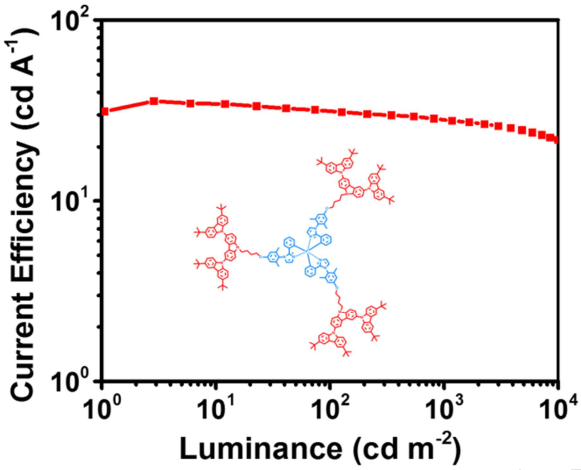

Solution processible imidiazole-based Ir dendrimers with oligocarbazole have been demonstrated for nondoped PhOLEDs, revealing a maximum current efficiency of 35.7 cd/A accompanied by a small efficiency roll-off at high luminance.

Solution Processible Imidazole-Based Iridium Dendrimers with Oligocarbazole for Nondoped Phosphorescent OLEDs

Mingming Zhang,[a,b] Xuefei Li,[a,b] Shumeng Wang,[a] Junqiao Ding,*[,a,b] Lixiang Wang*[,a,b]

[a] *State Key Laboratory of Polymer Physics and Chemistry, Changchun Institute of Applied Chemistry, Chinese Academy of Sciences, Changchun 130022, P. R. China*

[b] *University of Science and Technology of China, Hefei 230026, P. R. China*

Abstract

By introducing *t*-butyl- or methoxyl-containing oligocarbazole into the periphery of tris(mesityl-2-phenyl-1H-imidazole)iridium(III) [Ir(mpim)$_3$], two novel imidazole-based Ir dendrimers ^{t}Bu-D2-Ir(mpim)$_3$ and MeO-D2-Ir(mpim)$_3$ have been designed and synthesized through a convenient post-dendronization route. Due to the effective encapsulation, the intermolecular interactions and thus luminescence quenching in solid states is found to be gradually reduced following a sequence of Ir(mpim)$_3$ > MeO-D2-Ir(mpim)$_3$ > ^{t}Bu-D2-Ir(mpim)$_3$. Compared with the bare Ir(mpim)$_3$ core (Φ_{PL} = 0.38 and τ = 0.26 μs), accordingly, the film photoluminescence quantum yield and excited state lifetime are improved to 0.54 and 0.39 μs for MeO-D2-Ir(mpim)$_3$ and 0.88 and 1.09 μs for ^{t}Bu-D2-Ir(mpim)$_3$. When these developed Ir dendrimers are adopted as the emitting layer alone, ^{t}Bu-D2-Ir(mpim)$_3$ achieves an excellent nondoped device performance, revealing a maximum current efficiency as high as 35.7 cd/A (13.2%, 37.4 lm/W) together with Commission Internationale del_Eclairage coordinates of (0.21, 0.45). Even at a high luminance of 1000, 5000 and 10000 cd/m^2, it still remains to be 27.8, 24.7 and 21.8 cd/A, respectively, indicative of the gentle efficiency roll-off. The result clearly demonstrates the great potential of imidazole-based Ir dendrimers used for efficient nondoped phosphorescent organic light-emitting diodes.

Keywords: PhOLEDs; imidazole; Ir dendrimer; oligocarbazole; nondoped device

1. Introduction

Phosphorescent organic light-emitting diodes (PhOLEDs) capable of wet preparation have attracted much attention in recent years due to their good compability with low-cost, large-area and flexible flat-panel displays [1-4]. Besides small molecules [5, 6] and polymers [7, 8], dendrimers containing transition-metal complexes are believed to be a promising class of electroluminescent materials for solution processed PhOLEDs [9-16]. Such phosphorescent dendrimers have both the well-defined structures of small molecules and the excellent solution processibility of polymers. Most importantly, they can not only maintain the inherent emissive properties from cores, but also realize prohibited intermolecular interactions to reduce triplet-triplet annihilation (TTA) in neat films because of the characteristic shielding effect [17, 18]. Therefore, they are able to be independently used as the emitting layer (EML) to fabricate efficient nondoped devices without any additional host. In this case, the tedious doping technology and potential phase segregation would be avoided to enhance device performance including efficiency, lifetime and reproducibility [19-21].

Nowadays blue- [12-14, 22, 23], green- [16, 18, 24-29], yellow- [30] and red-emitting [31, 32] phosphorescent dendrimers with a self-host feature have been developed for high-performance nondoped PhOLEDs, where the outer dendrons act as the hosts and the inner core plays the same role as dopant. For example, with tris[2-(2,4-difluorophenyl)-pyridyl]iridium(III) [Ir(dfppy)$_3$] as the core and oligocarbazole as the dendron, a self-host blue Ir dendrimer B-G2 was demonstrated to reveal a continuous enhancement in the device efficiency with increasing doping concentration [10]. And the corresponding nondoped device was achieved without loss in efficiency, thus giving a state-of-art external quantum efficiency (EQE) of 15.3% (31.3 cd/A, 28.9 lm/W) and Commission Internationale del_Eclairage (CIE) coordinates of (0.16, 0.29). Furthermore, solution processed white OLEDs were realized by simply blending a yellow phosphor (iridium(III)[5-trifluoromethyl-2-(9,9-diethylfluoren-2-yl)pyridine]) [Ir(Flpy-CF_3)$_3$] into B-G2 [33]. Unlike the traditional host-based devices, the host-induced power efficiency losses could be eliminated, leading to an improved power efficiency of 58.8 lm/W along with CIE coordinates of (0.44, 0.45).

Albeit the successes, the adopted core in B-G2 consists of the electron-withdrawing F atom, which is proved to be readily cleaved to shorten the device lifetimes [34]. On the other hand, imidazole-based Ir complexes in absence of F, such as tris(mesityl-2-phenyl-1H-imidazole)iridium(III) [Ir(mpim)$_3$], turn out to be more stable than the F-containing counterparts [35, 36]. Meanwhile, they show red-shifted emissions towards a greenish-blue region, suitable for the fabrication of low driving voltage and power-efficient white OLEDs [37, 38]. With these considerations, here we further report imidazole-based Ir dendrimers ^{t}Bu-D2-Ir(mpim)$_3$ and MeO-D2-Ir(mpim)$_3$ by introducing different oligocarbazole dendrons into the periphery of Ir(mpim)$_3$ via a nonconjugated linkage (Figure 1). On the basis of a nondoped device configuration, a promising current efficiency as high as 35.7 cd/A (13.2%, 37.4 lm/W) is obtained. Even at a high luminance of 1000, 5000 and 10000 cd/m^2, it still remains to be 27.8, 24.7 and 21.8 cd/A, respectively, indicative of the gentle efficiency roll-off.

2. Results and discussion

2.1 Synthesis and characterization

A post-dendronization method similar to our previous work [16] is utilized for the convenient synthesis of the imidazole-based Ir dendrimers ^{t}Bu-D2-Ir(mpim)$_3$ and MeO-D2-Ir(mpim)$_3$. As depicted in Scheme 1, 4-bromo-2,6-dimethylaniline was firstly amidated with benzoyl chloride to afford N-(4-bromo-2,6-dimethylphenyl)benzamide (**1**), followed by a dehydro-cyclization. The resultant 1-(4-bromo-2,6-dimethylphenyl)-2-phenyl-1H-imidazole (**2**) was then converted to 1-(4-hydroxy-2,6-dimethylphenyl)-2-phenyl-1H-imidazole (**4**) after a successive bromide-to methoxyl conversion and demethylation under BBr_3. Subsequently, through a modified two-step complexation, the key intermediate HO-Ir(mpim)$_3$ functionalized with three reactive hydroxyl groups was successfully prepared in an acceptable yield of 38%. Finally, with the alkyl bromide oligocarbazole dendrons (^{t}Bu-D2-C4-Br and MeO-D2-C4-Br) in hand, a Williamson reaction was performed to easily produce the desired dendrimers ^{t}Bu-D2-Ir(mpim)$_3$ and MeO-D2-Ir(mpim)$_3$ in a high yield of 83-87%. Their molecular structures were well characterized using ^{1}H NMR, MALDI-TOF spectra and elemental analysis (Figure S1-S5). The total number of resonances in the ^{1}H NMR spectra of HO-Ir(mpim)$_3$, ^{t}Bu-D2-Ir(mpim)$_3$ and MeO-D2-Ir(mpim)$_3$ are equal to the number of resonances in a single C^N ligand, indicative of the inherent C_3 symmetry and facial isomer. Moreover, both ^{t}Bu-D2-Ir(mpim)$_3$ and MeO-D2-Ir(mpim)$_3$ are thermally stable, whose decomposition temperature (T_d, corresponding to a 5% weight loss) is detected to be 409 and 384 ^{o}C, respectively (Table 1 and Figure S6).

2.2 Electrochemical properties

The electrochemical properties of ^{t}Bu-D2-Ir(mpim)$_3$ and MeO-D2-Ir(mpim)$_3$ were investigated by cyclic voltammetry (CV) with ferrocene/ferrocenium (Fc/Fc$^+$) as the reference. During the sweeping in dichloromethane, they both show multiple oxidation processes with no reduction ones (Figure 2). Compared with Ir(mpim)$_3$, the first oxidation wave located at about -0.08 V can be assigned to the central Ir core, while the others at positive potentials are from the outer oligocarbazole dendrons. Accordingly, the highest occupied molecular orbital (HOMO) and lowest unoccupied molecular orbital (LUMO) energy levels of ^{t}Bu-D2-Ir(mpim)$_3$ and MeO-D2-Ir(mpim)$_3$ are estimated to be -4.72 eV and -2.10 eV, respectively, close to those of Ir(mpim)$_3$. The observation suggests that the incorporation of oligocarbazole dendrons does not affect the electrochemical behavior of the Ir core. In addition, we note that the second oxidation wave occurs at 0.53 V for ^{t}Bu-D2-Ir(mpim)$_3$ and 0.40 V for MeO-D2-Ir(mpim)$_3$. The ease oxidation of the methoxyl-containing oligocarbazole in MeO-D2-Ir(mpim)$_3$ relative to *t*-butyl-containing oligocarbazole in ^{t}Bu-D2-Ir(mpim)$_3$ is understandable when considering the stronger electron donating ability of methoxyl than *t*-butyl. According to the literature [13], this is favorable for the hole injection and transport in a dendritic Ir complex, which will be discussed below. Moreover, the oxidation processes of the methoxyl-containing oligocarbazole dendron and the Ir(mpim)$_3$ core may interact with each other (Figure S7), leading to the inferior reversibility and electrochemical stability of MeO-D2-Ir(mpim)$_3$ compared with ^{t}Bu-D2-Ir(mpim)$_3$.

2.3 Photophysical properties

Figure 3 shows the UV-Vis absorption spectra in dichloromethane and photoluminescence (PL) spectra in toluene and films for the imidazole-based Ir dendrimers compared with Ir(mpim)$_3$. As can be clearly seen, both ^{t}Bu-D2-Ir(mpim)$_3$ and MeO-D2-Ir(mpim)$_3$ exhibit two distinct bands including the weak absorption in the range of 325-450 nm and intense absorption below 325 nm. The first one is attributed to the metal-to-ligand charge-transfer (MLCT) transitions from the inner Ir core. And the second one is assigned to the ligand-centered (LC) transitions from the inner Ir core together with the π-π* transitions from the outer dendrons, whose absorbance is found to be greatly increased after the introduction of oligocarbazole. With respect to Ir(mpim)$_3$, additionally, their PL spectra in toluene remain nearly unchanged with a 0-0 emission at 470 nm and 0-1 emission at 496 nm. Given the nonconjugated linkage between dendron and core, the observed similarity is reasonable, suggesting that the inherent emission of the Ir core is independent of the peripheral dendrons in solutions.

However, different PL behaviors are observed ongoing from solutions to solid states. As for $Ir(mpim)_3$ without any dendrons, the PL spectrum moves to a longer wavelength accompanied by a significant enhancement of 0-1 and 0-2 emissions. In contrast, no obvious variation of the spectral profile and only a bathochromic shift of 8 and 14 nm are observed for ^{t}Bu-D2-$Ir(mpim)_3$ and MeO-D2-$Ir(mpim)_3$, respectively. Because of the encapsulation from the outer dendrons, the intermolecular interactions and thus luminescence quenching in neat films are found to be gradually decreased following a sequence of $Ir(mpim)_3$ > MeO-D2-$Ir(mpim)_3$ > ^{t}Bu-D2-$Ir(mpim)_3$. This is further verified by the transient PL spectra (Figure 4), in which the excited state lifetimes are determined to be 0.26, 0.39 and 1.09 μs for $Ir(mpim)_3$, MeO-D2-$Ir(mpim)_3$ and ^{t}Bu-D2-$Ir(mpim)_3$, respectively. And the film photoluminescence quantum yield (PLQY) is correspondingly up from 0.38 of $Ir(mpim)_3$ to 0.54 of MeO-D2-$Ir(mpim)_3$ and 0.88 of ^{t}Bu-D2-$Ir(mpim)_3$ (Table 1).

It should be noted that the encapsulation from methoxyl-containing oligocarbazole in MeO-D2-$Ir(mpim)_3$ is not as effective as that from *t*-butyl-containing oligocarbazole in ^{t}Bu-D2-$Ir(mpim)_3$. Besides the different steric hindrance between methoxyl and *t*-butyl, the triplet energy arrangement is tentatively responsible for the above phenomenon (Figure 5). Although they are both higher than that of the $Ir(mpim)_3$ core (2.63 eV), the triplet energy is reduced from 2.83 eV of *t*-butyl-containing oligocarbazole to 2.75 eV of methoxyl-containing oligocarbazole owing to the stronger electron donating ability of methoxyl than *t*-butyl. Thereby the possibility of the back triplet energy transfer from core to dendron may be increased

[39], leading to the reduced lifetime and PLQY of MeO-D2-Ir(mpim)$_3$ relative to ^{t}Bu-D2-Ir(mpim)$_3$.

2.4 Electroluminescence properties

To investigate the electroluminescence (EL) properties of ^{t}Bu-D2-Ir(mpim)$_3$ and MeO-D2-Ir(mpim)$_3$, nondoped PhOLEDs were fabricated with a configuration of ITO/PEDOT:PSS (40 nm)/Ir dendrimer (40 nm)/TSPO1 (5 nm)/TmPyPB (45 nm)/LiF (1 nm)/Al (Figure S8). Herein, PEDOT:PSS [poly(3,4-ethylenedioxythiophene:poly(styrenesulfonate)] serves as the hole-injection layer, whereas TSPO1 [diphenyl(4-(triphenylsilyl)phenyl)phosphine oxide] and TmPyPB [1,3,5-tri(m-pyrid-3-yl-phenyl)benzene] act as the exciton blocking layer and the electron-transporting layer, respectively. Similar to their PL counterparts, two developed imidazole-based Ir dendrimers both give bright greenish-blue EL solely from the central Ir core, and no emission residue from the peripheral dendrons is detected (Figure 6a). The related CIE coordinates are (0.21, 0.45) for ^{t}Bu-D2-Ir(mpim)$_3$ and (0.22, 0.47) for MeO-D2-Ir(mpim)$_3$.

As mentioned above, a better hole injection and transport can be anticipated in MeO-D2-Ir(mpim)$_3$ than in ^{t}Bu-D2-Ir(mpim)$_3$ because methoxyl-containing oligocarbazole has a shallow HOMO level compared to t-butyl-containing oligocarbazole. Therefore, the current density-voltage and luminance-voltage curves distinctly shift towards a lower driving voltage from ^{t}Bu-D2-Ir(mpim)$_3$ to MeO-D2-Ir(mpim)$_3$ (Figure 6b). For instance, the turn-on voltage at 1 cd/m^2 is down from 2.8 V to 2.4 V, which is even smaller than previously reported self-host blue Ir dendrimers.[11] In spite of this, a maximum current efficiency of 35.7 cd/A and 21.1 cd/A, a maximum power efficiency of 37.4 lm/W and 25.5 lm/W, and a peak EQE of 13.2% and 7.3% are realized for the nondoped devices of ^{t}Bu-D2-Ir(mpim)$_3$ and MeO-D2-Ir(mpim)$_3$, respectively (Figure 6c and 6d, Table 2). Compared with MeO-D2-Ir(mpim)$_3$, the superior device efficiency for ^{t}Bu-D2-Ir(mpim)$_3$ can be explained by the higher film PLQY originating from the effective encapsulation. Furthermore, ^{t}Bu-D2-Ir(mpim)$_3$ reveals a gentle efficiency roll-off, and its current efficiency slightly decays to 27.8, 24.7 and 21.8 cd/A at 1000, 5000 and 10000 cd/m^2, respectively. In view of the obtained promising performance, ^{t}Bu-D2-Ir(mpim)$_3$ may be also suitable for power-efficient white OLEDs without an additional host [33], which will be reported by our group in due course.

3. Conclusion

In summary, two novel imidazole-based Ir dendrimers have been designed and synthesized with Ir(mpim)$_3$ as the core and *t*-butyl- or methoxyl-containing oligocarbazole as the dendron. Benefiting from the reduced intermolecular interactions in solid states caused by the effective encapsulation, their film PLQYs and excited state lifetimes are improved obviously compared with the bare core. When a nondoped configuration is adopted, as a result, a promising current efficiency as high as 35.7 cd/A is realized associated with a gentle efficiency roll-off at high luminance. The result clearly demonstrates the great potential of imidazole-based Ir dendrimers used for efficient nondoped PhOLEDs.

4. Experimental section

General information: ^{1}H NMR spectra were measured on a Bruker Avance 400 NMR spectrometer. Elemental analysis was performed using a Bio-Rad elemental analysis system. MALDI/TOF (Matrix assisted laser desorption ionization/Time-of-flight) mass spectra were performed on AXIMA CFR MS apparatus (COMPACT) using 2-[(2E)-3-(4-tert-butylphenyl)-2-methylprop-2-enylidene]malononitrile (DCTB) as the matrix. Thermal properties of the dendrimers were analyzed with a Perkin-Elmer-TGA 7 instrument under nitrogen at a heating rate of 10 ^{o}C min^{-1}. UV-vis absorption and PL spectra were measured with a Perkin-Elmer Lambda 35 UV-vis spectrometer and a Perkin-Elmer LS 50B spectrofluorometer, respectively. Phosphorescence spectra of the oligocarbazole dendrons were measured at 77 K in a toluene solvent. The film PLQY was measured using an integrating sphere (Binson C9920-2) under N_2. The transient PL spectra were measured under a N_2 atmosphere and excited at a 375 nm with Edinburgh fluorescence spectrometer (FLS920). Following a biexponential fitting, the corresponding average lifetimes were estimated according to the equation: $\tau_{av} = (A_1\tau_1^2 + A_2\tau_2^2)/(A_1\tau_1 + A_2\tau_2)$. CV measurements were carried out in dichloromethane with a conventional three-electrode system consisting of a platinum working electrode, a platinum counter electrode, and an Ag/AgCl reference electrode. The supporting electrolyte was 0.1 M tetrabutylammonium perchlorate (n-Bu_4NClO_4). All potentials were calibrated against the Fc/Fc^+ couple. The HOMO levels were calculated according to the equation HOMO = -e(E_{ox}^{onset} + 4.8 V), where E_{ox}^{onset} is the onset value of the first oxidation wave. And the LUMO levels were calculated according to the equation LUMO = HOMO + E_g, where E_g is the optical bandgap estimated from the absorption onset.

Device fabrication and testing: To fabricate nondoped PhOLEDs, a 40 nm-thick PEDOT:PSS film was firstly deposited on the pre-cleaned and UVO-treated ITO-glass substrates (20 Ω per square). After baked at 120 ^oC for 40 min, then solutions of the Ir dendrimers in chlorobenzene were filtered through a filter (0.45 μm) and spin coated on PEDOT:PSS as the EML. The thickness of the EML was about 40 nm after annealing at 120 ^oC for 30 min. Subsequently, the substrate was transferred to a vacuum thermal evaporator and a 5 nm-thick film of TSPO1 and a 45 nm-thick film of TmPyPB was evaporated on top of the EML at a base pressure less than 10^{-6} Torr (1 Torr = 133.32 Pa). Finally, 1 nm LiF and 100 nm Al were deposited successively as the cathode through a shadow mask with an array of 14 mm^2 openings. The current density-voltage-luminance characteristics were measured using a Keithley source measurement unit (Keithley 2400 and Keithley 2000) calibrated by a silicon photodiode. The EL spectra were measured using a SpectraScan PR650 spectrophotometer. All the measurements were carried out at room temperature under ambient conditions. EQE was calculated from the luminance, current density and EL spectra assuming a Lambertian distribution.

Synthesis: All chemicals and reagents used in this work were received from commercial sources without further purification. Solvents for chemical synthesis were purified according to the standard procedures. ^{t}Bu-D2-C4-Br and MeO-D2-C4-Br were prepared according to our previous work [10, 40].

N-(4-bromo-2,6-dimethylphenyl)benzamide (**1**): The mixture of 4-bromo-2,6-dimethylaniline (5.0 g, 25 mmol) and pyridine (4.0 g, 50 mmol) in 30 mL CH_2Cl_2 was stirred, and cooled to 0 ^{o}C under ice bath. To this solution, benzoyl chloride (3.5 g, 25 mmol) in 10 mL CH_2Cl_2 was added dropwisely under argon atmosphere, followed by a stirring overnight at room temperature. After the reaction completed, the solvent was removed by vacuum distillation. Then the residue was washed by petroleum ether, and dried in vacuum to give the crude product **1**, which was directly used for the next step without further purification.

1-(4-bromo-2,6-dimethylphenyl)-2-phenyl-1H-imidazole (**2**): **1** (7.6 g, 25 mmol) dissolved in 50 mL xylene was added PCl_5 (7.8 g, 37.5 mmol) slowly. The mixture was refluxed overnight under argon. When the reaction completed, the solvent was removed by vacuum distillation, followed by adding 50 mL THF and cooling to 0 ^{o}C. Then 2,2-dimethoxyethan-1-amine (6.6 g, 62.5 mmol) in THF(10 mL) was added dropwise under argon atmosphere, and the mixture was stirred for 8 h at room temperature. The mixture was added 30 mL 6 M HCl, and further heated to reflux overnight. After cooling to room temperature, the mixture was poured into saturated

$NaHCO_3$ solution, and extracted with CH_2Cl_2. The organic phase was washed with water and dried over anhydrous sodium sulfate. Finally, the residue was purified by column chromatography on silica gel with petroleum ether: ethyl acetate = 4:1 as the eluent to give the product **2** (4.7 g, 58 %). ^{1}H NMR (400 MHz, d6-DMSO): δ = 7.50 (s, 2H), 7.29 (s, 6H), 7.28 (d, *J* = 1.2 Hz, 1H), 7.26 (d, *J* = 1.2 Hz, 1H), 1.88 (s, 6H).

1-(4-methoxy-2,6-dimethylphenyl)-2-phenyl-1H-imidazole (**3**): Methanol (20 mL) in a flask was cooled to 0 ^{o}C with ice bath before sodium (2.1 g, 92 mmol) was added. The ice water bath was removed, and the mixture was stirred until the sodium disappeared. Then DMF (20 mL), CuI (3.5 g, 18.4 mmol) and **2** (3.0 g, 9.2 mmol) were added into this sodium methoxide solution. The resulting mixture was heated to reflux for 4 h under argon atmosphere. The hot mixture was rapidly filtered, and the filtrate was poured into water and extracted with CH_2Cl_2. The combined organic layers were neutralized with 1 M HCl, followed by washing with water and brine, drying with Na_2SO_4. After solvent removal, the residue was purified by silica gel column chromatography using petroleum ether:ethyl acetate = 10:1 as eluent to give the product **3** (1.8 g, 72%). ^{1}H NMR (400 MHz, d6-DMSO): δ = 7.31 (ddd, *J* = 8.4, 5.6, 2.5 Hz, 2H), 7.27 (dd, *J* = 6.6, 3.3 Hz, 3H), 7.22 (s, 1H), 7.20 (s, 1H), 6.81 (s, 2H), 3.78 (s, 3H), 1.88-1.81 (m, 6H).

1-(4-hydroxy-2,6-dimethylphenyl)-2-phenyl-1H-imidazole (**4**): A solution of **3** (2.7 g, 9.7 mmol) in dry CH_2Cl_2 (50 mL) was cooled to 0 ^oC, and BBr_3 (2.7 mL 1 M solution in CH_2Cl_2, 29 mmol) was added dropwise. After stirring for 4 h at room temperature, the reaction was carefully quenched with methanol. The solvent was removed by vacuum distillation. Then the residue was recrystallization by acetone to give the pure product **4** as white solid (2.3 g, 90%). ^1H NMR (400 MHz, d6-DMSO): δ = 9.65 (s, 1H), 7.35-7.31 (m, 2H), 7.27 (dd, *J* = 6.5, 2.8 Hz, 3H), 7.20 (d, *J* = 1.2 Hz, 1H), 7.17 (d, *J* = 1.1 Hz, 1H), 6.60 (s, 2H), 1.79 (s, 6H).

tris(2-(1-(4-hydroxy-2,6-dimethylphenyl)-1H-imidazol-2-yl)phenyl)iridium (HO-Ir(mpim)$_3$): $IrCl_3 \cdot 3H_2O$ (1.0 g, 2.83 mmol) and **4** (1.87 g, 7.08 mmol) were added in a 30 mL mixture of 2-methoxyethanol (15 mL) and water (15 mL). The mixture was refluxed for 24 h and then poured into water. The solid was collected by filtration and dried in vacuum to give the chloro-bridged dimer. Next, the crude dimer, silver trifluoroacetate (1.25 g, 5.66 mmol), **4** (1.5 g, 5.66 mmol), ethelene glycol monophenyl ether (15 mL) and ethylene glycol (15 mL) were heated to 120 ^oC for 24 h under argon atmosphere. After cooling to room temperature, the solvent was removed by vacuum distillation. The pure product HO-Ir(mpim)$_3$ (1.1 g) was obtained in a total yield of 38% by chromatography on silica gel using petroleum ether : ethyl acetate = 4:1 as eluent. ^1H NMR (400 MHz, d6-DMSO): δ = 9.75 (s, 1H), 7.12 (s, 1H), 6.72 (d, *J* = 7.5 Hz, 1H), 6.68 (d, *J* = 2.7 Hz, 2H), 6.57 (s, 1H), 6.47 (t, *J* = 7.3 Hz, 1H), 6.37 (t, *J* = 7.4 Hz, 1H), 6.13 (d, *J* = 7.7 Hz, 1H), 1.93 (s, 3H), 1.74 (s, 3H).

General Procedure for the Synthesis of ^{t}Bu-D2-Ir(mpim)$_3$ and MeO-D2-Ir(mpim)$_3$: A mixture of ^{t}Bu-D2-C4-Br or MeO-D2-C4-Br (3.5 equiv.), HO-Ir(mpim)$_3$ (1 equiv.) and cesium carbonate (5 equiv.) in DMF was heated to 80 ^{o}C under argon atmosphere for 24 h. The mixture was cooled to room temperature, poured into water and extracted with ethyl acetate. The combined organic layers were washed with brine and water, followed by drying with Na_2SO_4. After the solvent removal, the desired dendrimers were obtained by silica gel column chromatography using petroleum ether: ethyl acetate = 6:1 as eluent for ^{t}Bu-D2-Ir(mpim)$_3$ and toulene : ethyl acetate = 10:1 as eluent for MeO-D2-Ir(mpim)$_3$.

^{t}Bu-D2-Ir(mpim)$_3$ (530 mg, 87%): ^{1}H NMR (400 MHz, C_6D_6): δ = 8.49 (s, 4H), 8.01 (d, *J* = 1.8 Hz, 2H), 7.65-7.47 (m, 10H), 7.25-7.18 (m, 3H), 6.99 (s, 1H), 6.85 (t, *J* = 6.4 Hz, 1H), 6.72 (d, *J* = 6.3 Hz, 1H), 6.69 (d, *J* = 7.2 Hz, 1H), 6.64 (d, *J* = 1.9 Hz, 1H), 6.57 (s, 1H), 6.34 (s, 1H), 3.41 (d, *J* = 5.5 Hz, 2H), 2.03 (s, 3H), 1.73 (s, 4H), 1.65 (s, 5H), 1.45 (s, 36H). MALDI-TOF (m/z): 3308.8 [M^+]. Anal. calcd. For $C_{219}H_{228}IrN_{15}O_3$: C, 79.46; H, 6.94; N, 6.35; Found: C, 79.40; H, 7.20; N, 6.21.

MeO-D2-Ir(mpim)$_3$ (485 mg, 83%): ^{1}H NMR (400 MHz, C_6D_6): δ = 7.89 (s, 2H), 7.74 (s, 4H), 7.53 (s, 1H), 7.46 (d, *J* = 8.6 Hz, 2H), 7.36 (d, *J* = 8.8 Hz, 4H), 7.19 (d, *J* = 8.9 Hz, 6H), 6.97 (s, 1H), 6.83 (d, *J* = 6.9 Hz, 1H), 6.69 (t, *J* = 9.6 Hz, 2H), 6.61 (s, 1H), 6.55 (s, 1H), 6.33 (s, 1H), 3.92 (s, 2H), 3.58 (s, 12H), 3.43 (s, 2H), 2.01 (s, 3H), 1.76 (d, *J* = 6.5 Hz, 2H), 1.71 (s, 3H), 1.51 (s, 2H). MALDI-TOF (m/z): 2996.2 [M^+].

Anal. calcd. For $C_{183}H_{156}IrN_{15}O_{15}$: C, 73.33; H, 5.25; N, 7.01; Found: C, 73.24; H, 5.45; N, 6.98.

Author Information:

Corresponding authors: junqiaod@ciac.ac.cn; lixiang@ciac.ac.cn

Acknowledgements

The authors acknowledge the financial support from the National Key Research and Development Program (2016YFB0401301), the 973 Project (2015CB655001) and the National Natural Science Foundation of China (Nos. 51573183 and 51873205).

References:

[1] C. Liu, Q. Fu, Y. Zou, C. Yang, D. Ma, J. Qin, Low Turn-on Voltage, High-Power-Efficiency, Solution-Processed Deep-Blue Organic Light-Emitting Diodes Based on Starburst Oligofluorenes with Diphenylamine End-Capper to Enhance the HOMO Level, Chem. Mater., 26 (2014) 3074-3083.

[2] C.-F. Liu, Y. Jiu, J. Wang, J. Yi, X.-W. Zhang, W.-Y. Lai, W. Huang, Star-Shaped Single-Polymer Systems with Simultaneous RGB Emission: Design, Synthesis, Saturated White Electroluminescence, and Amplified Spontaneous Emission, Macromolecules, 49 (2016) 2549-2558.

[3] M.A. Baldo, D.F. O'Brien, Y. You, A. Shoustikov, S. Sibley, M.E. Thompson, S.R. Forrest, Highly efficient phosphorescent emission from organic electroluminescent

devices, Nature, 395 (1998) 151.

[4] H. Zheng, Y. Zheng, N. Liu, N. Ai, Q. Wang, S. Wu, J. Zhou, D. Hu, S. Yu, S. Han, W. Xu, C. Luo, Y. Meng, Z. Jiang, Y. Chen, D. Li, F. Huang, J. Wang, J. Peng, Y. Cao, All-solution processed polymer light-emitting diode displays, Nat. Commun., 4 (2013) 1971.

[5] T. Giridhar, T.-H. Han, W. Cho, C. Saravanan, T.-W. Lee, S.-H. Jin, An Easy Route to Red Emitting Homoleptic IrIII Complex for Highly Efficient Solution-Processed Phosphorescent Organic Light-Emitting Diodes, Chem. – Eur. J., 20 (2014) 8260-8264.

[6] N. Aizawa, Y.-J. Pu, M. Watanabe, T. Chiba, K. Ideta, N. Toyota, M. Igarashi, Y. Suzuri, H. Sasabe, J. Kido, Solution-processed multilayer small-molecule light-emitting devices with high-efficiency white-light emission, Nat. Commun., 5 (2014) 5756.

[7] S.-y. Shao, J.-q. Ding, L.-x. Wang, Research Progress on Electroluminescent Polymers, Acta. Polym. Sin., (2018) 198-216.

[8] S.-Y. Shao, J.-Q. Ding, L.-X. Wang, New applications of poly(arylene ether)s in organic light-emitting diodes, Chin. Chem. Lett., 27 (2016) 1201-1208.

[9] P.L. Burn, S.C. Lo, I.D.W. Samuel, The Development of Light-Emitting Dendrimers for Displays, Adv. Mater., 19 (2007) 1675-1688.

[10] D. Xia, B. Wang, B. Chen, S. Wang, B. Zhang, J. Ding, L. Wang, X. Jing, F. Wang, Self-host blue-emitting iridium dendrimer with carbazole dendrons: nondoped phosphorescent organic light-emitting diodes, Angew. Chem., Int. Ed., 53 (2014)

1048-1052.

[11] X. Yang, G. Zhou, W.Y. Wong, Functionalization of phosphorescent emitters and their host materials by main-group elements for phosphorescent organic light-emitting devices, Chem. Soc. Rev., 44 (2015) 8484-8575.

[12] Y. Wang, Y. Lu, B. Gao, S. Wang, J. Ding, L. Wang, X. Jing, F. Wang, Single molecular tuning of the charge balance in blue-emitting iridium dendrimers for efficient nondoped solution-processed phosphorescent OLEDs, Chem. Commun., 52 (2016) 11508-11511.

[13] Y. Wang, S. Wang, J. Ding, L. Wang, X. Jing, F. Wang, Dendron engineering in self-host blue iridium dendrimers towards low-voltage-driving and power-efficient nondoped electrophosphorescent devices, Chem. Commun., 53 (2017) 180-183.

[14] Y. Wang, S. Wang, S. Shao, J. Ding, L. Wang, X. Jing, F. Wang, Synthesis and properties of greenish-blue-emitting iridium dendrimers with N-phenylcarbazole-based polyether dendrons by a post-dendronization route, Dalton Trans., 44 (2015) 1052-1059.

[15] W.-Y. Wong, C.-L. Ho, Functional metallophosphors for effective charge carrier injection/transport: new robust OLED materials with emerging applications, J. Mater. Chem. C, 19 (2009) 4457.

[16] Y. Wang, S. Wang, N. Zhao, B. Gao, S. Shao, J. Ding, L. Wang, X. Jing, F. Wang, Facile synthesis of self-host functional iridium dendrimers up to the fourth generation with N-phenylcarbazole-based polyether dendrons for non-doped phosphorescent organic light-emitting diodes, Polym. Chem., 6 (2015) 1180-1191.

[17] J. Ding, B. Wang, Z. Yue, B. Yao, Z. Xie, Y. Cheng, L. Wang, X. Jing, F. Wang, Bifunctional Green Iridium Dendrimers with a “Self-Host” Feature for Highly Efficient Nondoped Electrophosphorescent Devices, Angew. Chem., Int. Ed., 121 (2009) 6792-6794.

[18] L. Chen, Z. Ma, J. Ding, L. Wang, X. Jing, F. Wang, Self-host heteroleptic green iridium dendrimers: achieving efficient non-doped device performance based on a simple molecular structure, Chem. Commun., 47 (2011) 9519-9521.

[19] H.A. Al Attar, A.P. Monkman, Dopant Effect on the Charge Injection, Transport, and Device Efficiency of an Electrophosphorescent Polymeric Light-Emitting Device, Adv. Funct. Mater., 16 (2006) 2231-2242.

[20] Y.-Y. Noh, C.-L. Lee, J.-J. Kim, K. Yase, Energy transfer and device performance in phosphorescent dye doped polymer light emitting diodes, J. Chem. Phys., 118 (2003) 2853-2864.

[21] S. Reineke, K. Walzer, K. Leo, Triplet-exciton quenching in organic phosphorescent light-emitting diodes with Ir-based emitters, Phys. Rev. B, 75 (2007) 125328.

[22] S.-C. Lo, R.N. Bera, R.E. Harding, P.L. Burn, I.D.W. Samuel, Solution-Processible Phosphorescent Blue Dendrimers Based on Biphenyl-Dendrons and Fac-tris(phenyltriazolyl)iridium(III) Cores, Adv. Funct. Mater., 18 (2008) 3080-3090.

[23] S.-C. Lo, R.E. Harding, C.P. Shipley, S.G. Stevenson, P.L. Burn, I.D.W. Samuel, High-Triplet-Energy Dendrons: Enhancing the Luminescence of Deep Blue

Phosphorescent Iridium(III) Complexes, J. Am. Chem. Soc., 131 (2009) 16681-16688.

[24] J. Ding, J. Gao, Y. Cheng, Z. Xie, L. Wang, D. Ma, X. Jing, F. Wang, Highly Efficient Green-Emitting Phosphorescent Iridium Dendrimers Based on Carbazole Dendrons, Adv. Funct. Mater., 16 (2006) 575-581.

[25] S.C. Lo, T.D. Anthopoulos, E.B. Namdas, P.L. Burn, I.D.W. Samuel, Encapsulated Cores: Host-Free Organic Light-Emitting Diodes Based on Solution-Processible Electrophosphorescent Dendrimers, Adv. Mater., 17 (2005) 1945-1948.

[26] W. Tian, Q. Qi, B. Song, C. Yi, W. Jiang, X. Cui, W. Shen, B. Huang, Y. Sun, A bipolar homoleptic iridium dendrimer composed of diphenylphosphoryl and diphenylamine dendrons for highly efficient non-doped single-layer green PhOLEDs, J. Mater. Chem. C, 3 (2015) 981-984.

[27] J. Ding, J. Lü, Y. Cheng, Z. Xie, L. Wang, X. Jing, F. Wang, Effect of ancillary ligands on the properties of heteroleptic green iridium dendrimers functionalized with carbazole dendrons, J. Organomet. Chem., 694 (2009) 2700-2704.

[28] T. Qin, J. Ding, L. Wang, M. Baumgarten, G. Zhou, K. Müllen, A Divergent Synthesis of Very Large Polyphenylene Dendrimers with Iridium(III) Cores: Molecular Size Effect on the Performance of Phosphorescent Organic Light-Emitting Diodes, J. Am. Chem. Soc., 131 (2009) 14329-14336.

[29] L. Chen, Z. Ma, J. Ding, L. Wang, X. Jing, F. Wang, Effect of dendron generation on properties of self-host heteroleptic green light-emitting iridium

dendrimers, Org. Electron., 13 (2012) 2160-2166.

[30] M. Zhu, J. Zou, X. He, C. Yang, H. Wu, C. Zhong, J. Qin, Y. Cao, Triphenylamine Dendronized Iridium(III) Complexes: Robust Synthesis, Highly Efficient Nondoped Orange Electrophosphorescence and the Structure–Property Relationship, Chem. Mater., 24 (2012) 174-180.

[31] J. Ding, J. Lü, Y. Cheng, Z. Xie, L. Wang, X. Jing, F. Wang, Solution-Processible Red Iridium Dendrimers based on Oligocarbazole Host Dendrons: Synthesis, Properties, and their Applications in Organic Light-Emitting Diodes, Adv. Funct. Mater., 18 (2008) 2754-2762.

[32] L. Zhao, S. Wang, J. Lü, J. Ding, L. Wang, Solution processable red iridium dendrimers containing oligocarbazole dendrons for efficient nondoped and doped phosphorescent OLEDs, J. Mater. Chem. C, 5 (2017) 9753-9760.

[33] S. Wang, Q. Yang, B. Zhang, L. Zhao, D. Xia, J. Ding, Z. Xie, L. Wang, Improving the Power Efficiency of Solution-Processed Phosphorescent WOLEDs with a Self-Host Blue Iridium Dendrimer, Adv. Optical Mater., 5 (2017) 1700514.

[34] V. Sivasubramaniam, F. Brodkorb, S. Hanning, H.P. Loebl, V. van Elsbergen, H. Boerner, U. Scherf, M. Kreyenschmidt, Fluorine cleavage of the light blue heteroleptic triplet emitter FIrpic, J. Fluorine Chem., 130 (2009) 640-649.

[35] Y. Kwon, S.H. Han, S. Yu, J.Y. Lee, K.M. Lee, Functionalized phenylimidazole-based facial-homoleptic iridium(iii) complexes and their excellent performance in blue phosphorescent organic light-emitting diodes, J. Mater. Chem. C, 6 (2018) 4565-4572.

[36] Y. Zhang, J. Lee, S.R. Forrest, Tenfold increase in the lifetime of blue phosphorescent organic light-emitting diodes, Nat. Commun., 5 (2014) 5008.

[37] K. Udagawa, H. Sasabe, C. Cai, J. Kido, Low-driving-voltage blue phosphorescent organic light-emitting devices with external quantum efficiency of 30%, Adv. Mater, 26 (2014) 5062-5066.

[38] K. Udagawa, H. Sasabe, F. Igarashi, J. Kido, Simultaneous Realization of High EQE of 30%, Low Drive Voltage, and Low Efficiency Roll-Off at High Brightness in Blue Phosphorescent OLEDs, Adv. Optical Mater., 4 (2016) 86-90.

[39] R.J. Holmes, S.R. Forrest, Y.J. Tung, R.C. Kwong, J.J. Brown, S. Garon, M.E. Thompson, Blue organic electrophosphorescence using exothermic host–guest energy transfer, Appl. Phys. Lett., 82 (2003) 2422-2424.

[40] S. Shao, S. Wang, X. Xu, Y. Yang, J. Lv, J. Ding, L. Wang, X. Jing, F. Wang, Realization of high-power-efficiency white electroluminescence from a single polymer by energy-level engineering, Chem. Sci., (2018) DOI: 10.1039/C8SC03753A.

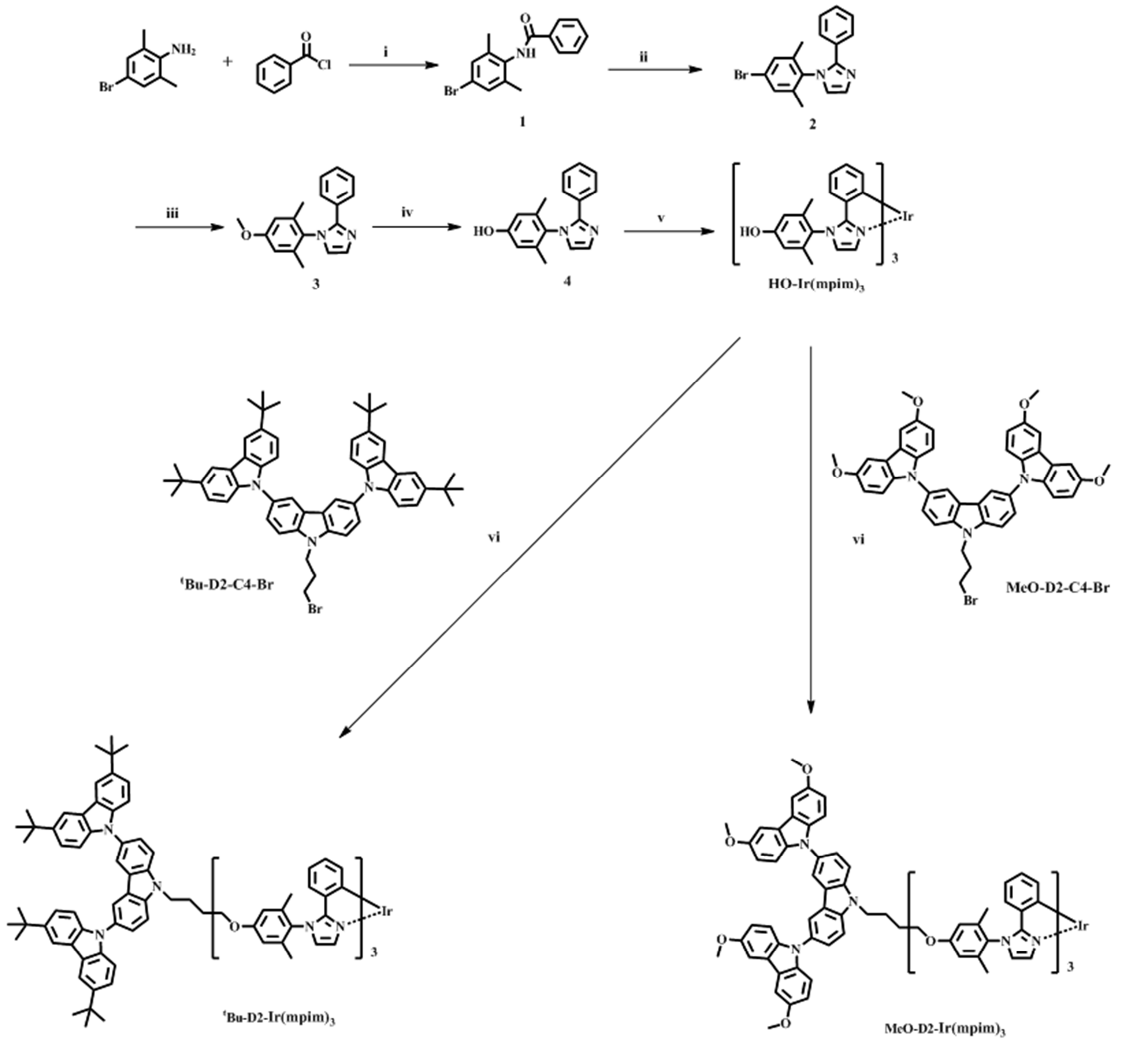

Scheme 1. Synthetic route of the imidazole-based Ir dendrimers ^{t}Bu-D2-Ir(mpim)$_3$ and MeO-D2-Ir(mpim)$_3$. Reagents and conditions: (i) pyridine, CH_2Cl_2, 0 ^{o}C; (ii) PCl_5, xylene, reflux, and then 2,2-dimethoxyethan-1-amine, THF, 0 ^{o}C; (iii) CH_3OH, Na, CuI, DMF, reflux; (iv) BBr_3, CH_2Cl_2, 0 ^{o}C; (v) $IrCl_3 \cdot 3H_2O$, water, 2-methoxyethanol, reflux, and then silver trifluoroacetate, **4**, ethelene glycol monophenyl ether, ethylene glycol, 120 ^{o}C; (vi) Cs_2CO_3, DMF, 80 ^{o}C.

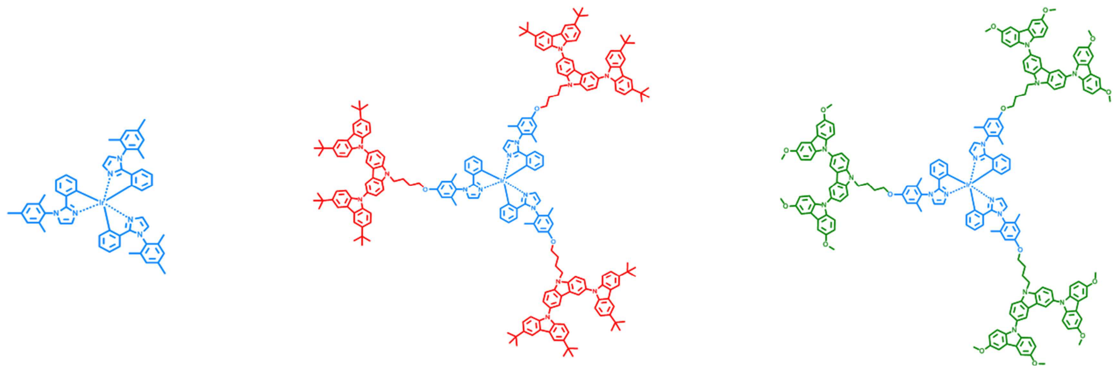

Ir(mpim)$_3$ **^{t}Bu-D2-Ir(mpim)$_3$** **MeO-D2-Ir(mpim)$_3$**

Figure 1. Molecular structures of the imidazole-based Ir dendrimers ^{t}Bu-D2-Ir(mpim)$_3$ and MeO-D2-Ir(mpim)$_3$ together with the core Ir(mpim)$_3$.

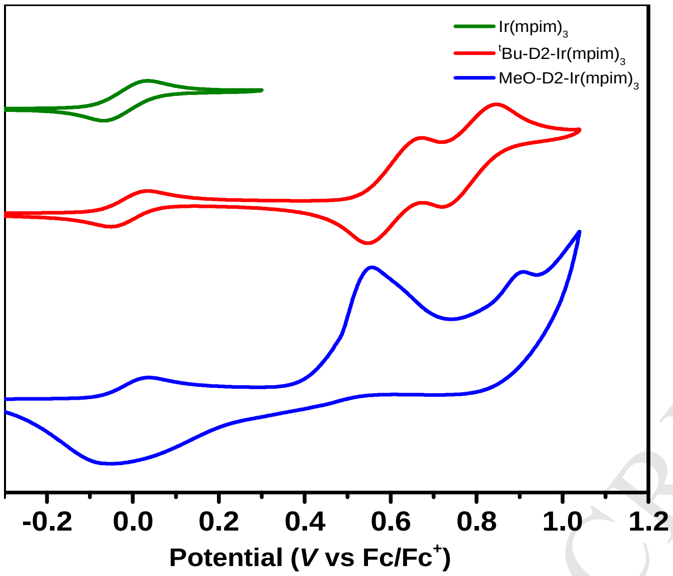

Figure 2. CV plots for ^{t}Bu-D2-Ir(mpim)$_3$ and MeO-D2-Ir(mpim)$_3$ compared with Ir(mpim)$_3$.

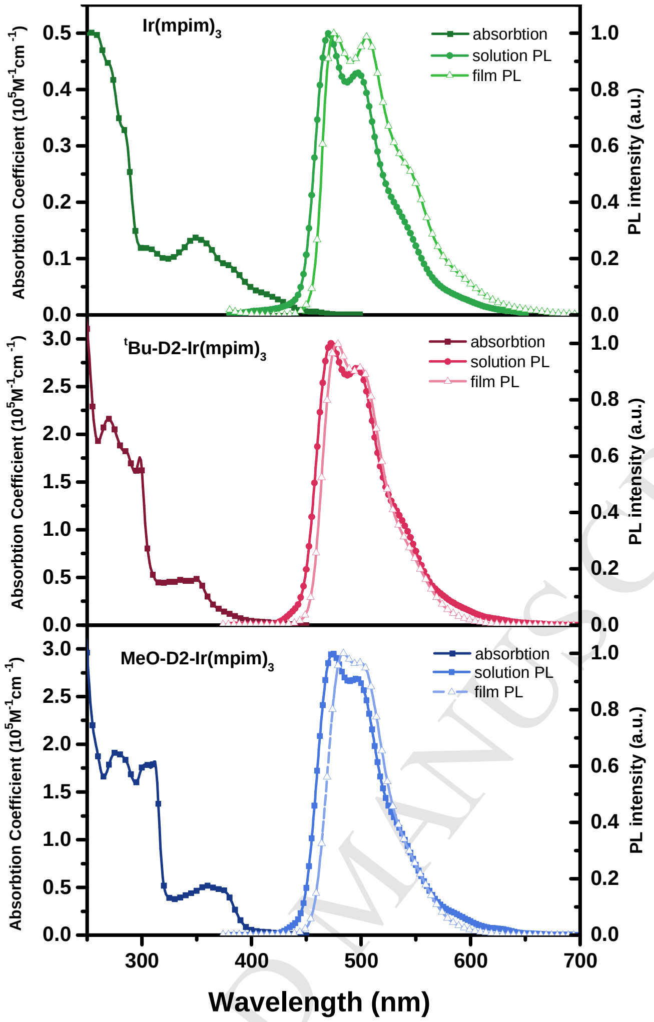

Figure 3. UV-Vis absorption spectra in dichloromethane and PL spectra in both toluene and films for Ir(mpim)$_3$, ^{t}Bu-D2-Ir(mpim)$_3$ and MeO-D2-Ir(mpim)$_3$.

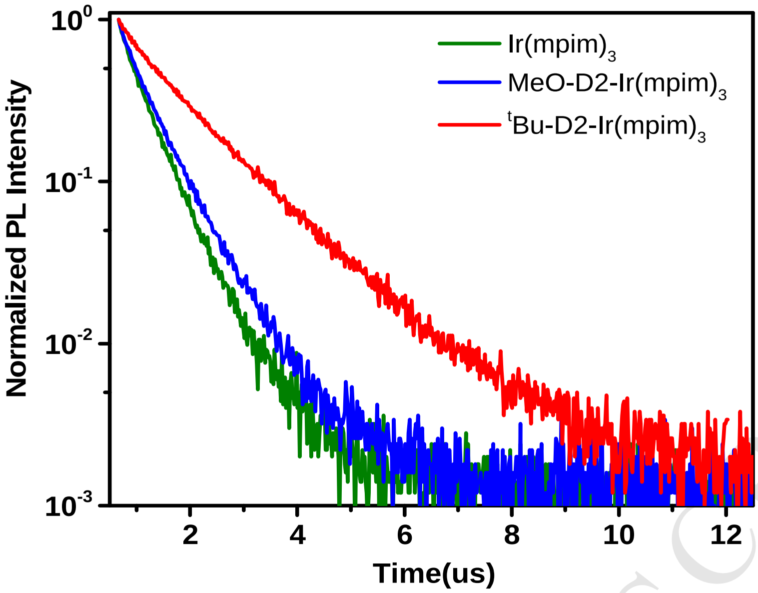

Figure 4. Transient PL spectra for thin films of Ir(mpim)$_3$, ^{t}Bu-D2-Ir(mpim)$_3$ and MeO-D2-Ir(mpim)$_3$.

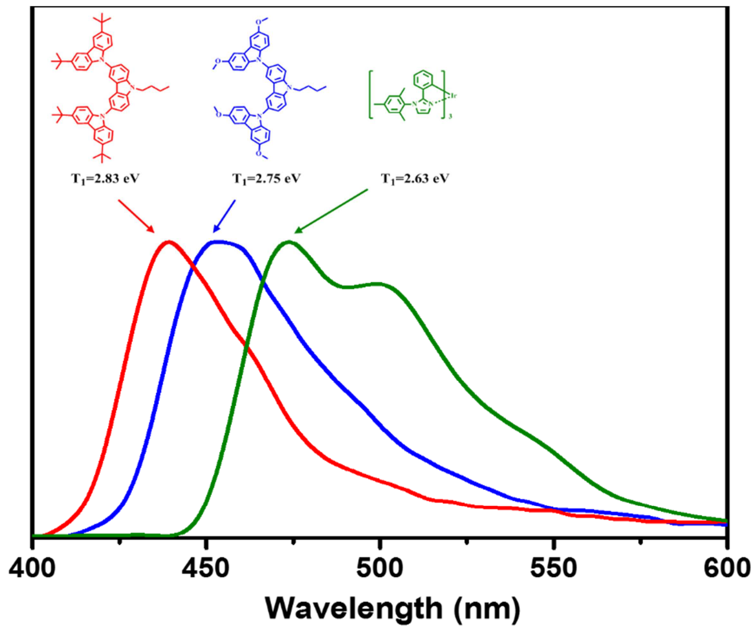

Figure 5. Phosphorescent spectra for the oligocarbazole dendrons compared with the Ir core.

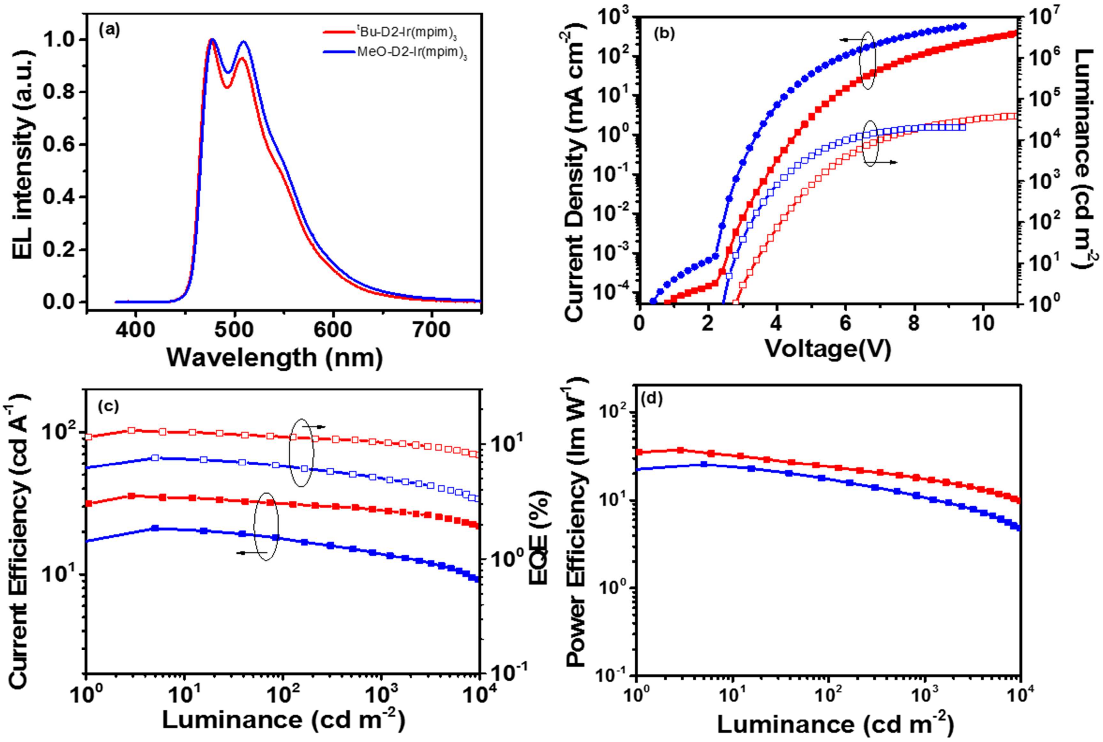

Figure 6. Nondoped device performance for ^{t}Bu-D2-Ir(mpim)$_3$ and MeO-D2-Ir(mpim)$_3$: (a) EL spectra at a driving voltage of 6 V; (b) current density-voltage-luminance curves; (c) current efficiency and EQE as a function of luminance; (d) power efficiency as a function of luminance.

Table 1. Photophysical, electrochemical and thermal properties for ^{t}Bu-D2-Ir(mpim)$_3$ and MeO-D2-Ir(mpim)$_3$ compared with Ir(mpim)$_3$.

	λ_{abs} (logε)^{a} [nm]	λ_{em} ^{b} [nm]	λ_{em} ^{c} [nm]	Φ_{PL} ^{d}	τ ^{e} [μs]	E_g ^{f} [eV]	HOMO ^{g} [eV]	LUMO ^{g} [eV]	T_d [^{o}C]
Ir(mpim)$_3$	251 (0.5), 270 (0.4), 284 (0.3), 308 (0.1), 350 (0.1), 380 (0.1)	471, 497	475, 505	0.38	0.26	2.63	-4.74	-2.11	370
^{t}Bu-D2-Ir(mpim)$_3$	269 (5.3), 285 (1.8), 298 (5.2), 349 (4.7)	470, 496	478, 499	0.88	1.09	2.62	-4.72	-2.10	409
MeO-D2-Ir(mpim)$_3$	276 (5.3), 303 (5.3), 312 (5.3), 359 (4.7), 373 (4.7)	470, 496	484, 499	0.54	0.39	2.63	-4.72	-2.09	384

^{a}Measured in 10^{-5} M dichloromethane; ^{b}Measured in 10^{-5} M toluene; ^{c}Measured in neat films; ^{d}Measured in neat films using an integrating sphere under N_2; ^{e}Measured in neat films under N_2 with an excitation of 375 nm; ^{f}Optical band gap estimated from the absorption onset; ^{g}HOMO = -e(E_{ox}^{onset} + 4.8 V), LUMO = HOMO + E_g, where E_{ox}^{onset} is the onset value of the first oxidation wave.

Table 2. Nondoped device performance for the imidazole-based Ir dendrimers ^{t}Bu-D2-Ir(mpim)$_3$ and MeO-D2-Ir(mpim)$_3$.

Device	V_{on} [a] [V]	L_{max} [cd m^{-2}]	η_c [b] [cd A^{-1}]	η_p [b] [lm W^{-1}]	EQE [b] [%]	CIE [c] [x,y]
^{t}Bu-D2-Ir(mpim)$_3$	2.8	20020	35.7/27.8	37.4/16.8	13.2/10.2	(0.21, 0.45)
MeO-D2-Ir(mpim)$_3$	2.4	38700	21.1/14.4	25.5/11.1	7.3/5.2	(0.22, 0.47)

[a]Turn-on voltage at a brightness of 1 cd m^{-2}; [b]Maximum values and data at 1000 cd m^{-2} for current efficiency (η_c), power efficiency (η_b) and EQE, respectively; [c]CIE at 1000 cd m^{-2}.

Highlights

1. Two imidazole-based Ir dendrimers capable of solution processing have been developed for efficient nondoped PhOLEDs.
2. Due to the effective encapsulation, the intermolecular interactions and thus luminescence quenching in solid states is found to be gradually reduced for the developed Ir dendrimers.
3. Solution processed nondoped devices achieve a promising current efficiency as high as 35.7 cd/A (13.2%, 37.4 lm/W) together with a gentle efficiency roll-off at high luminance.